Room-temperature controllable fabrication of silver nanoplates reduced by aniline†

Jinling Song, Ying Chu,* Yang Liu, Lili Li and Wendong Sun

Received (in Cambridge, UK) 15th October 2007, Accepted 3rd January 2008
First published as an Advance Article on the web 21st January 2008
DOI: 10.1039/b715884j

Ag nanoplates are the first generated by the reductant aniline in the presence of poly(vinyl pyrrolidone) (PVP) at room temperature without stirring in the reaction process.

The intrinsic properties of metal nanoparticles are mainly determined by their size, shape, composition, crystallinity and structure. For example, the surface plasmon resonance of metal particles is strongly shape-dependent, which results from the collective oscillation of the electrons in the conduction band from one surface of the particle to the other.[1,2] Notably, silver or gold nanoplates are capable of generating maximum electromagnetic-field enhancement and make these nanoparticles suitable for surface-enhanced Raman scattering (SERS) detection or other spectroscopic techniques.[3] Recently, a number of methods have been developed for the synthesis of silver and gold nanostructures to fine tune shapes, including nanoparticles,[4] triangular plates,[5] cubes,[6] belts,[7] wires,[8] rods,[9] and branched multipods.[10] Up to now, the corresponding synthetic methods include microwave (MW),[11–13] hydrothermal,[14] reflux,[6,15,16] photoinduced method[3,17] and so on.[18–21] However, these methods demand rigorous conditions in order to achieve the reaction. Here we demonstrate a mild wet-chemical route to the synthesis of Ag nanoplates obtained using aniline as reductant at room temperature.‡ Compared to the reports referred above, our reaction does not demand any additional energy such as heating or agitation. Furthermore, in our work, the synthesis of Ag nanoplates reduced by aniline is the first reported. The amine is the key factor for the controllable synthesis of triangular Ag nanoplates at room temperature.

A typical X-ray diffraction (XRD) pattern of the as-prepared samples is shown in Fig. S1 (ESI†). The peaks are assigned to diffraction from the (111), (200), (220), (311) and (222) planes of face-centered cubic (fcc) Ag, respectively. (JCPDS, 4-783). Fig. 1(a) and (b) show transmission electron microscopy (TEM) and scanning electron microscopy (SEM) images of the sample by typical synthesis, respectively. As observed in Fig. 1, the sample is composed of many large nanoplates and a few polyhedral nanoparticles. The average edge length and thickness are about 550 and 24 nm, respectively, while the average size of the polyhedral nanoparticles are about 100 nm. From Fig. 1(a), some randomly distributed and continuous lines are seen across the faces of the nanoplates leading to a reduction in thickness in these regions.

Fig. 2(a) and (b) show high-magnification TEM images of nanoplates and polyhedron nanoparticles. The inset of Fig. 2(a) shows the diffraction pattern recorded by aligning the electron beam perpendicular to the triangular facets of an individual nanoplate. The hexagonal symmetry of the diffraction spots indicates the silver nanoplate is a single crystal. The inset of Fig. 2(b) shows an electron-diffraction pattern taken from the nanoparticles. The rings correspond to diffraction from the (111), (200), (220) and (311) planes of fcc Ag. The electron diffraction patterns show that the Ag nanoplates are singe-crystal and Ag nanoparticles are polycrystals. When the reduction is slow enough, the reaction is kinetically controlled: the seeds with stacking defects will nucleate and then grow into nanoplates,[22] but an extremely slow reaction would continuously generate Ag atoms over a long period of time, and thus induce the coexistence of single crystals and polycrystals of Ag metal, so resulting in polydispersity. Fig. 2(c) shows a high-resolution TEM image of an individual Ag nanoplate. The fringe space is estimated to be 0.25 nm, which is close to 1/3 of the *d*-value of the (422) reflection.

To study the growth mechanism of the silver nanoplates, a series of experiments were carried out for different periods of time. Fig. S2(a)–(c), ESI† show TEM images of samples synthesized for 2, 4 and 6 h, respectively. As shown in Fig. S2, the samples consisted of nanoparticles and nanoplates with sharp edges and corners. At $t = 2$ h (Fig. S2(a)), the average edge length of the nanoplates and nanoparticles were around

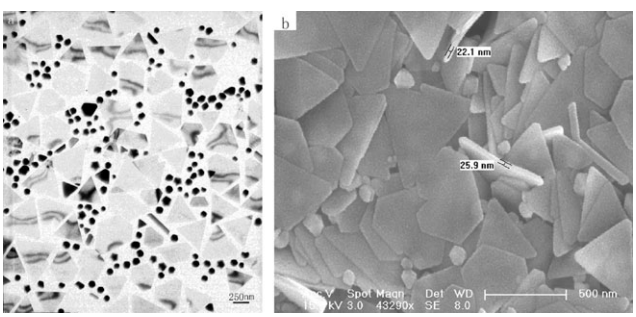

Fig. 1 TEM (a) and SEM (b) images of Ag nanoplates synthesized by the typical route with $[AgNO_3]$: [An] ratio of 2 : 1.

Department of Chemistry, Northeast Normal University, Jinlin, Changchun 130024, (P.R. China). E-mail: chuying@nenu.edu.cn

† Electronic supplementary information (ESI) available: Fig. S1–S6, showing the XRD image, TEM images of samples at different stages and UV-vis spectrum, TEM images of Ag nanoplates synthesized at different $[AgNO_3]$: [An] ratios, TEM and SEM images of Ag nanoplates synthesized in dark room, TEM image of Ag synthesized without PVP, TEM image of Ag reduced by hydrazine hydrate instead of aniline. See DOI: 10.1039/b715884j

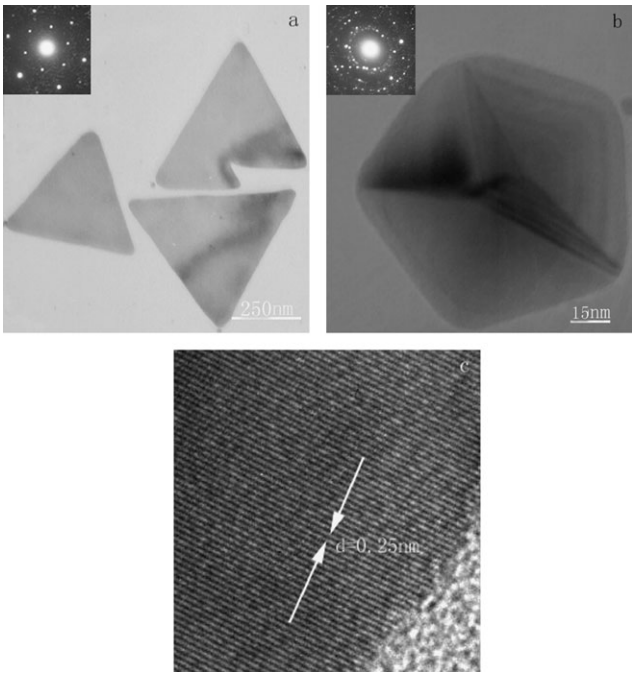

Fig. 2 High-magnification TEM images of Ag nanoplates with $[AgNO_3]$: [An] ratio of 2 : 1 (a) and polyhedron nanoparticles (b). The insets show the corresponding electron diffraction patterns. (c) High-resolution TEM images of the edge of the triangular nanoplates in the sample shown in Fig. 1.

250 and 45 nm, respectively. With the reaction proceeding for t = 4 h (Fig. S2(b)), the nanoplates and nanoparticles grew a little larger than that of 2 h. At t = 6 h (Fig. S3(c)), the nanoplates and nanoparticles increased to 500 nm and 90 nm in size, respectively. When the reaction time reached 24 h, the nanoplates and the nanoparticles were about 550 and 100 nm, respectively. The ratio in size of nanoplates to nanoparticles was about 5.5 during the whole reaction process. Fig. S2(d) shows the UV-vis spectra of Ag nanoparticle aqueous suspensions obtained at different stages of the reaction. The spectra show mainly two absorption peaks at about 335 and 420-490 nm, which can be assigned to quadrupole plasmon resonances and out-of plane dipole, respectively. The positions of the extinction peaks were gradually red-shifted to the near-IR region of the electromagnetic spectrum with increasing particle size.[23] Because of the polydispersity of the nanostructures, broad peaks can be only observed from the UV-vis spectra. The results are consistent with the TEM images of Fig. S2, ESI.†

The $[AgNO_3]$: [An] ratio was found to have a significant influence on the morphology of the Ag nanoplates. When $[AgNO_3]$: [An] was between 1 : 2 and 4 : 1, the edge length of Ag nanoplates decreased with increasing $[AgNO_3]$: [An] ratio. Fig. S3(a), (b), 1 and 3(c) show the Ag nanoplates synthesized at $[AgNO_3]$: [An] ratio of 1 : 2, 1 : 1, 2 : 1 and 4 : 1, respectively, with the same concentration of $AgNO_3$ as used for the sample in Fig. 1. When the $[AgNO_3]$: [An] ratio is high, $AgNO_3$ as the oxidant can induce rapid reaction, so the speed of nucleation is faster than that of growth. After the same reaction time, the size of Ag nanoplates synthesized at high $[AgNO_3]$: [An] is smaller than that of low ratio.

To investigate the influence of light on the synthesis of Ag nanoplates, we carried out the controllable reactions in a dark environment with other conditions unchanged. Fig. S4(a) and (b), ESI,† show the TEM and SEM images of the sample synthesized in the dark room, revealing the edge length as about 500 nm. As reported earlier, triangular seeds with small sizes (5–10 nm) were formed in the early stage of their photoinduced conversion process. The application of continuous irradiation helped to digest the spherical colloids into small clusters, which then grew on the tiny triangular seeds, leading to the formation of larger nanoplates.[5] However, compared to the TEM images of the samples synthesized by exposure to natural light, there are nearly no difference. The results indicate that light is not the determining factor for the growth of the Ag nanoplates. We suppose that the amine plays an important role in the formation of the Ag nanoplates.

In order to investigate the function of the amine group, we carried out the following controllable experiments in the absence of PVP with other conditions unchanged. The resulting sample consisted of polyhedron nanoparticles shown in Fig. S5, ESI,† which were similar to the nanoparticles synthesized in a typical reaction, and the nanoparticles tended to aggregate. Seen carefully, we can observe a triangular silver particle which is indicated by an arrow in Fig. S5. From the results we can conclude that aniline as the reductant is able to lead to Ag metal from $AgNO_3$, but alone can not direct nanoparticles into nanoplates effectively. Xia *et al*. synthesized Ag triangular nanoplates with high purity by heating an aqueous solution of $AgNO_3$ and PVP to 60 °C in a capped vial.[15] However, when we carried out the reaction without aniline in the presence of PVP at room temperature with other conditions unchanged, the reaction hardly occurred, and Ag nanoplates could not be obtained. Some papers reported the preparation of silver nanoplates in the presence of PVP without other reductant.[11,15,24] but the silver nanoplates were obtained with a large amount of PVP on heating. Zhang *et al*. developed the small biomolecule (glycyl glycine)-directed synthesis of single-crystalline silver nanoplates at 160 °C for 24 h,[14] They believe that glycyl glycine could play roles both as reducing agent and as capping ligand at relatively high concentrations in the synthesis of silver nanoplates in solution. We believe this report provides further proof of the amine group as the reductant. Lee and his group obtained Ag nanoplates at room temperature with pyridine in the presence of PVP.[25] We suppose that amine group from pyridine is the key to ensure that the reaction can be completed under mild conditions.

Here we also carried out the synthesis of Ag by hydrazine hydrate ($N_2H_4{\cdot}H_2O$) reduction instead of aniline with other conditions unchanged. When a solution of $AgNO_3$ was poured into the reaction system, the mixed solution rapidly turned green. Fig. S6, ESI,† shows the TEM image of the sample. The sample consists mostly of nanoparticles ($d \sim 50$ nm) and a few nanoplates. We believe that the reaction proceeded rapidly in the presence of hydrazine, and the kinetics of nucleation can not be controlled effectively. The amount of silver source is certain, while the speed of nucleation is much faster than that of growth, and finally the growth of nanoparticles to nanoplates is restrained. Hydrazine can thus reduce $AgNO_3$ to

nanoplates but the fast reaction is disadvantageous to the growth of Ag nanoplates.

From these results, we can further confirm that aniline is a suitable reductant *via* electron transfer from the amine group to cationic silver ions in the mild reaction system where the NH_2 of aniline can direct the growth of Ag to polyhedra as well as triangular Ag. The reaction mechanism is similar to that reported.[26,27] In our reaction system, PVP as an important capping agent can be adsorbed preferentially on certain crystal facets protecting the Ag nanoparticles from aggregation, and promote the synthesis of Ag nanoplates.

In summary, Ag nanoplates with controllable edge lengths have been fabricated by the redox reaction between $AgNO_3$ and aniline. In the reaction, aniline was as the reductant with PVP as the dispersive agent, directing the growth of silver nanoplates. There are two special novelties in the reaction: (a) this is the first report of the synthesis of Ag nanoplates reduced by aniline; (b) the reaction condition is mild and occurs at room temperature; (c) in the whole reaction process no stirring or imput of any energy is required. We found that the size of Ag nanoplates depended upon the reaction time and the ratio of [$AgNO_3$] : [An]. Light is not necessary for the formation of the nanoplates, with the reducing amine group key to forming Ag nanoplates. This simple synthetic strategy can also be applied to synthesize other noble metals, and our subsequent work will focus on this.

We thank the National Natural Science Foundation of China (20573017) and Analysis and Testing Foundation of Northeast Normal University for financial support.

Notes and references

‡ A typical synthesis is as follows: Aniline monomer was distilled under reduced pressure and stored in the refrigerator. Other reagents were used as received without further treatment. The typical synthesis of silver triangular nanoplates was as follows: 0.4 g PVP (M_w = 30 000) was dissolved into 10 mL ethanol, and then 100 μL aniline was added into the above solution and magnetic stirring at room temperature, until there were no aniline droplets in the system. 10 mL of an aqueous solution of 0.2 M $AgNO_3$ was rapidly added into the clear solution. The reaction was carried out under magnetic stirring for 30 s, and then kept standing for 24 h at room temperature. A series of color changes was observed during the course of the reaction. The solution turned brick-red, pale yellow, and then green eventually. At different stages of the reaction, samples were taken from the mixture using a glass pipette, centrifuged, and then washed with water several times to remove excess PVP for UV-vis characterization. A number of reactions were carried out under the same conditions but stopped after different periods of time. The Ag samples for XRD and SEM characterization were prepared by placing several drops of the suspension on a glass substrate and allowing the solvent to slowly evaporate at room temperature. The samples were characterized by X-ray powder diffraction (XRD) on a Rigaku X-ray diffractometer with Cu-Kα radiation (λ = 1.5406 Å). The morphology and size of as-obtained product were observed by transmission electron microscopy (TEM, Hitachi H-800) and field-emission scanning electron microscopy (FE-SEM, JEOL, 7500B). High-resolution transmission electron microscope and selected area electron diffraction (SAED) were performed with a transmission electron microscope (JEOL JEM-2010, 200 kV). UV-vis absorption spectra were recorded on a SHIMADZU UV-2550 UV-visible spectrophotometer using 1 cm quartz absorption cell.

1 (*a*) G. Schmidt and L. F. Chi, *Adv. Mater.*, 1998, **10**, 515; (*b*) R. D. Theys and G. Sosnovsky, *Chem. Rev.*, 1997, **97**, 83; (*c*) S. A. Maier, M. L. Brongersma, P. G. Kik, S. Meltzer, A. A. G. Requicha and H. A. Atwater, *Adv. Mater.*, 2001, **13**, 1501; (*d*) P. V. Kamat, *J. Phys. Chem. B*, 2002, **106**, 7729; (*e*) C. B. Murray, S. Sun, H. Doyle and T. Betley, *MRS Bull.*, 2001, **26**, 985; (*f*) M.-P. Pileni, *Adv. Funct. Mater.*, 2001, **11**, 323; (*g*) M. D. Malinsky, K. L. Kelly, G. C. Schatz and R. P. Van Duyne, *J. Am. Chem. Soc.*, 2001, **123**, 1471.

2 M. Chen and L. Gao, *Inorg. Chem.*, 2006, **45**, 5145.

3 (*a*) W. H. Yang, G. C. Schatz and R. P. Van Duyne, *J. Chem. Phys.*, 1995, **103**, 869; (*b*) K. L. Kelly, E. Coronado, L. L. Zhao and G. C. Schatz, *J. Phys. Chem. B*, 2003, **107**, 668.

4 Y. Wang and H. Yang, *Chem. Commun.*, 2006, 2545.

5 R. Jin, Y. Cao, C. A. Mirkin, K. L. Kelly, G. G. Schatz and J. G. Zheng, *Science*, 2001, **294**, 1901.

6 (*a*) Y. Sun and Y. Xia, *Science*, 2002, **298**, 2176; (*b*) R. Jin, S. Egusa and N. F. Scherer, *J. Am. Chem. Soc.*, 2004, **126**, 9900; (*c*) T. K. Sau and C. J. Murphy, *J. Am. Chem. Soc.*, 2004, **126**, 8648; (*d*) F. Kim, S. Connor, H. Song, T. Kuykendall and P. Yang, *Angew. Chem.*, 2004, **116**, 3759; (*e*) F. Kim, S. Connor, H. Song, T. Kuykendall and P. Yang, *Angew. Chem., Int. Ed.*, 2004, **43**, 3673.

7 Y. Sun, B. Mayers and Y. Xia, *Nano Lett.*, 2003, **3**, 675.

8 (*a*) Y. Sun, B. Mayers, T. Herricks and Y. Xia, *Nano Lett.*, 2003, **3**, 955; (*b*) Y. Sun, Y. Yin, B. Mayers, T. Herricks and Y. Xia, *Chem. Mater.*, 2002, **14**, 4736; (*c*) Y. Sun, B. Mayers and Y. Xia, *Adv. Mater.*, 2003, **15**, 641; (*d*) D. Zhang, L. Qi, J. Ma and H. Cheng, *Chem. Mater.*, 2001, **13**, 2753.

9 (*a*) N. R. Jana, L. Gearheart and C. J. Murphy, *J. Phys. Chem. B*, 2001, **105**, 4065; (*b*) C. J. Murphy and N. R. Jana, *Adv. Mater.*, 2002, **14**, 80; (*c*) F. Kim, J. H. Song and P. Yang, *J. Am. Chem. Soc.*, 2002, **124**, 14316.

10 (*a*) E. Hao, R. C. Bailey, G. C. Schartz, J. T. Hupp and S. Li, *Nano Lett.*, 2004, **4**, 327; (*b*) S. Chen, Z. L. Wang, J. Ballato, S. H. Foulger and D. L. Carroll, *J. Am. Chem. Soc.*, 2003, **125**, 186.

11 R. He, X. Qian, J. Yin and Z. J. Zhu, *J. Mater. Chem.*, 2002, **12**, 3783.

12 T. Yamamoto, H. Yin, Y. Wada, T. Kitamura, T. Sakata, H. Mori and S. Yanagida, *Bull. Chem. Soc. Jpn.*, 2004, **77**, 757.

13 M. Tsuji, M. Hashimoto, Y. Nishizawa and T. Tsuji, *Chem. Lett.*, 2003, **32**, 1114.

14 J. Yang, L. Lu, H. Wang, W. Shi and H. Zhang, *Cryst. Growth Des.*, 2006, **6**, 2155.

15 I. Washio, Y. Xiong, Y. Yin and Y. Xia, *Adv. Mater.*, 2006, **18**, 1745.

16 Y. Chen, X. Gu, C. G. Xie, Z. Y. Jiang, Z. X. Xie and C. J. Lin, *Chem. Commun.*, 2005, 4181.

17 Y. Sun and Y. Xia, *Adv. Mater.*, 2003, **15**, 695.

18 S. Chen and D. L. Carroll, *Nano Lett.*, 2002, **2**, 1003.

19 S. Chen, Z. Fan and D. L. Carroll, *J. Phys. Chem. B*, 2002, **106**, 10777.

20 M. Maillard, S. Giorgio and M.-P. Pileni, *Adv. Mater.*, 2002, **14**, 1084.

21 I. Pastoriza-Santos and L. M. Liz-Marzán, *Nano Lett.*, 2002, **2**, 903.

22 Y. Xiong, I. Washio, J. Chen, H. Cai, Z.-Y. Li and Y. Xia, *Langmuir*, 2006, **22**, 8563.

23 S. Chen, Z. Fan and D. L. Carroll, *J. Phys. Chem. B*, 2002, **106**, 10777.

24 I. Pastoriza-Santos and L. M. Liz-Marzán, *Langmuir*, 2002, **18**, 2888.

25 T. C. Deivaraj, N. L. Lala and J. Y. Lee, *J. Colloid Interface Sci.*, 2005, **289**, 402.

26 K. Jang, S. Y. Kim, K. H. Park, E. Jang, S. Jun and S. U. Son, *Chem. Commun.*, 2007, 4474.

27 J. D. S. Newman and G. J. Blanchard, *Langmuir*, 2006, **22**, 5882.